

Quantitative texture analysis in the prediction of IDH status in low-grade gliomas



Asgeir Store Jakola^{a,b,c,*,1}, Yi-Hua Zhang^{d,e,1}, Anne J. Skjulsvik^{f,g}, Ole Solheim^{c,h,i}, Hans Kristian Bø^{j,k}, Erik Magnus Berntsen^{i,k}, Ingerid Reinertsen^{h,l}, Sasha Gulati^{c,i}, Petter Förander^m, Torkel B. Brismar^{d,e}

^a Department of Neurosurgery, Sahlgrenska University Hospital, Gothenburg, Sweden

^b Institute of Neuroscience and Physiology, Sahlgrenska Academy, Gothenburg, Sweden

^c Department of Neurosurgery, St.Olavs University Hospital, Olav Kyrres Gate, 7006 Trondheim, Norway

^d Department of Radiology, Karolinska University Hospital (Huddinge), Stockholm, Sweden

^e Division of Medical Imaging and Technology, Department of Clinical Science, Intervention and Technology (CLINTEC), Karolinska Institute, Stockholm, Sweden

^f Department of Pathology, St.Olavs University Hospital, Trondheim, Norway

^g Department of Laboratory Medicine, Children's and Women's Health, Norwegian University of Science and Technology, Trondheim, Norway

^h National Norwegian Advisory Unit for Ultrasound and Image Guided Therapy, St.Olavs University Hospital, 7006 Trondheim Norway

ⁱ Department of Neuromedicine and Movement Science, Medical Faculty, Norwegian University of Science and Technology, 7491 Trondheim, Norway

^j Department of Radiology and Nuclear medicine, St.Olavs University Hospital, Olav Kyrres Gate, 7006 Trondheim, Norway

^k Department of Circulation and Medical Imaging, Faculty of Medicine and Health Sciences, Norwegian University of Science and Technology, Trondheim, Norway

^l Department of Medical Technology, SINTEF, Trondheim, Norway

^m Department of Neurosurgery, Karolinska University Hospital, Stockholm, Sweden

ARTICLE INFO

Keywords:

Classification

Glioma

IDH

Radiobiology

ABSTRACT

Objectives: Molecular markers provide valuable information about treatment response and prognosis in patients with low-grade gliomas (LGG). In order to make this important information available prior to surgery the aim of this study was to explore if molecular status in LGG can be discriminated by preoperative magnetic resonance imaging (MRI).

Patients and methods: All patients with histopathologically confirmed LGG with available molecular status who had undergone a preoperative standard clinical MRI protocol using a 3T Siemens Skyra scanner during 2008–2015 were retrospectively identified. Based on Haralick texture parameters and the segmented LGG FLAIR volume we explored if it was possible to predict molecular status.

Results: In total 25 patients (nine women, average age 44) fulfilled the inclusion parameters. The textural parameter homogeneity could discriminate between LGG patients with *IDH* mutation (0.12, IQR 0.10–0.15) and *IDH* wild type (0.07, IQR 0.06–0.09, $p = 0.005$). None of the other four analyzed texture parameters (energy, entropy, correlation and inertia) were associated with molecular status. Using ROC curves, the area under curve for predicting *IDH* mutation was 0.905 for homogeneity, 0.840 for tumor volume and 0.940 for the combined parameters of tumor volume and homogeneity. We could not predict molecular status using the four other chosen texture parameters (energy, entropy, correlation and inertia). Further, we could not separate LGG with *IDH* mutation with or without 1p19q codeletion.

Conclusions: In this preliminary study using Haralick texture parameters based on preoperative clinical FLAIR sequence, the homogeneity parameter could separate *IDH* mutated LGG from *IDH* wild type LGG. Combined with tumor volume, these diagnostic properties seem promising.

* Corresponding author at: Department of Neurosurgery, Sahlgrenska University Hospital, Blå stråket 5, 41345 Gothenburg, Sweden.

E-mail addresses: legepost@gmail.com (A.S. Jakola), yi-hua.zhang@ki.se (Y.-H. Zhang), anne.j.skjulsvik@ntnu.no (A.J. Skjulsvik), ole.solheim@ntnu.no (O. Solheim), hanskrb@gmail.com (H.K. Bø), erik.berntsen@ntnu.no (E.M. Berntsen), ingerid.reinertsen@sintef.no (I. Reinertsen), sasha.gulati@ntnu.no (S. Gulati), petter.forander@karolinska.se (P. Förander), torkel.brismar@gmail.com (T.B. Brismar).

¹ Shared first authorship.

<https://doi.org/10.1016/j.clineuro.2017.12.007>

Received 9 November 2017; Received in revised form 30 November 2017; Accepted 4 December 2017

Available online 05 December 2017

0303-8467/ © 2017 The Authors. Published by Elsevier B.V. This is an open access article under the CC BY-NC-ND license (<http://creativecommons.org/licenses/by-nc-nd/4.0/>).

1. Introduction

Low-grade glioma (LGG) is a relative rare intracranial neoplasm with an incidence of 1/100,000/year [1]. The median age of diagnosis is typically around 40, thus affecting otherwise healthy and young adults. It is not recommended to rely solely on diagnostic imaging, and the final diagnosis is usually based on histopathological assessment after surgery (biopsy or resection) [2].

The clinical heterogeneity within LGGs is remarkable. Low-grade gliomas are currently subclassified based on molecular markers, and *IDH* status (wild-type or mutated) together with 1p19q codeletion status now provides improved stratification and information about the underlying molecular profile [3]. It has even been suggested that *IDH* wild type (*IDHwt*), although morphologically a LGG, resembles glioblastoma from a molecular and clinical point of view.

Much data from routine anatomical MRI images are not quantitatively analyzed in regular clinical practice and this is also true for patients with LGG [4]. Consequently, there are numerous variables to be explored involving image intensity, shape and texture [5]. A study in lung-, head and neck cancer patients demonstrated that quantitative data from regular CT scans provided promising prognostic capabilities [5]. There are several reports on machine-learning techniques and multivariable imaging prediction models demonstrating prognostic capabilities using either routine MRI or special MRI sequences in high-grade glioma patients [6–9]. In a recent report on patients with high-grade gliomas researchers found that quantitative data from a combination of MRI with metabolic information and anatomical MRI could predict molecular status – hence provide non-invasive prognostic information [10]. Also, analysis of MRI from routine sequences with respect to glioma image heterogeneity has been able to reliably separate high-grade gliomas from LGG [11]. Taking it further, studies in LGG using a radiomics approach for *IDH* prediction have demonstrated promising results, especially when deep learning was applied [12,13]. Thus, it is likely that molecular status and prognosis in LGG patients can be predicted from MRI phenotypes.

Based on our previous clinical research in LGGs we have clinical and imaging data available, in addition to molecular profile [14]. In this group of patients we now explore textural parameters from anatomical MRIs using quantitative radiology to potentially predict molecular status and/or malignant transformation.

2. Material and methods

2.1. Patients

This is a retrospective study including patients with newly diagnosed and histopathologically verified supratentorial diffuse LGG in the time period from 2008 to 2016 with available digital preoperative 3T MRI images from Siemens Skyra scanner (Siemens, Erlangen, Germany). All patients were treated at St.Olavs hospital (Trondheim, Norway). Clinical and radiological data was retrieved from medical journals and earlier research projects. End of follow-up was 01st January 2016.

2.2. Radiology

For textural analyses 3D Fluid Attenuated Inversion Recovery (FLAIR) acquisitions with 1.00 mm slices and no inter-slice gap were used. Echo time, repetition time, inversion time and flip angle (TE/TR/TI/FA) was 389-394/5000/1800/120, thus with only slight variation in TE. In addition, T1 weighted images with gadolinium (gadoterate meglumine) were available for the conventional clinical description (e.g. concerning contrast enhancement), but not for the quantitative radiology. These were done as 3D gradient echo sequences with 1.00 mm slices and TE/TR/TI/FA being 2.92/2300/1100/8 or 2.96/2000/1100/8 or 3.16/1900/900/9. Both FLAIR and T1 sequences were done with

1.00 × 1.00 mm pixel spacing in a 256 × 256 matrix.

All follow-up MRI exams until reoperation were reviewed according to the criteria from the Response Assessment in Neuro-Oncology (RANO) group [15]. Follow-up MRI-exams were performed every 6 months, with shorter intervals of 2–3 months if unclear findings or possible sign of progression, and with intervals of up to 12 months after years of stable disease and no remaining FLAIR-abnormalities.

2.3. Image interpretation

A radiologist experienced with LGG assessment and segmentation (H.K.B) performed the semiquantitative data interpretation and did the tumor segmentation in 3D Slicer as previously described [16]. He was blinded for clinical result and molecular status while evaluating the following: contrast enhancement (no, patchy, nodular and ring-like), corpus callosum involvement (yes, no), tumor borders, main tumor side, volume in milliliters, and mass effect (no, mild, conspicuous). Tumor borders were radiological classified as 1) well-defined when the border between tumor and normal appearing brain was sharp; 2) partially absent (vague) when this border was still visible, but more diffuse; and 3) absent when tumor growth was very diffuse and this border was hardly possible to establish [16].

2.4. Texture analysis

Radiologists familiar with quantitative radiology (T.B.B and Y-H.Z) analyzed images after the segmentation procedure as described above. Haralick textural features were extracted from the segmented tumor volume in the MR image material [17]. The analysis was limited to energy, entropy, homogeneity, inertia and correlation, as previous studies have shown some features to be redundant [18]. Also, textural features have shown potential using quantitative radiology to predict *IDH* mutation in LGG previously [13]. Each feature was calculated based on the grey level co-occurrence matrices (GLCM) computed for all voxels in the segmented tumor volume. Each texture feature describes a relation of voxels with their local neighborhood, as detailed in Table 1. The signal intensities in the MR image data was rescaled to 0–256 grey levels for GLCM calculations. The GLCM was computed using 256 bins and using offsets in all 26 directions. The texture features were computed using an in-house written plug-in for ImageJ 1.50e [19].

Table 1
Description and equation of texture analysis parameters.

Energy	Describes the similarity of voxels in the region	$\sum_{i,j} p(i, j)^2$
Entropy	Describes the disorder in the distribution of gray levels in the region.	$-\sum_{i,j} p(i, j) \log(p(i, j))$
Correlation	Describes the correlation between voxel pairs in the region	$\sum_{i,j} \frac{(i - \mu_x)(j - \mu_y)}{\sigma_x \sigma_y} p(i, j)$
Homogeneity (Inverse Difference Moment)	Describes the homogeneity of the co-occurrence pairs	$\sum_{i,j} \frac{1}{1 + (i - j)^2} p(i, j)$
Inertia (Contrast)	Describes the variation in signal intensities	$\sum_{i,j} (i - j)^2 p(i, j)$

i and *j* refers to the bins in the grey level co-occurrence matrices, *p*(*i,j*) to the value of the marginal-probability at point (*i,j*).

2.5. Molecular markers

The *IDH* mutational status and 1p19q codeletion status were analyzed as previously described in detail [14].

2.6. Ethics

The regional ethical committee of Central Norway approved this project (reference 2016/1377). All patients have provided written informed consent.

2.7. Statistics

Data are presented as median values (interquartile range, IQR). Mean difference was tested using Mann-Whitney *U* test with tie correction. Statistical significance was defined at a level of $p < 0.05$. Statistical analysis was done using R 3.2.3, Vienna, Austria.

3. Results

In total, 25 patients fulfilled the inclusion criteria. Of those nine were women and average age was 44. In total, 20 patients had *IDH* mutation and 5 were *IDH* wild type. For additional details, see Table 2.

3.1. Quantitative radiology and *IDH* mutation status

Imaging characteristics and quantitative MRI data are presented in Table 3. The textural parameter homogeneity was significantly different depending on *IDH* mutation status, as shown in Fig. 1. A descriptive presentation of individual patients in relation to molecular profile (i.e. *IDHwt*, *IDHmut*, *IDHmut* and 1p19q codeletion) is presented in Fig. 2. In addition, imaging examples of low- and high homogeneity are presented in Fig. 3. Other textural parameters showed no significant correlations to *IDH* mutation status. ROC curves for *IDH* mutation status showed good classification results for both homogeneity and tumor volume, and when combining homogeneity and tumor volume in correlation to *IDH* status by logistic regression of a generalized linear model, we demonstrate good classification results as seen in Fig. 4. The area under the curve (AUC) for predicting *IDH* mutation was 0.905 for homogeneity, 0.840 for tumor volume and 0.940 for the combined parameters of tumor volume and homogeneity.

Table 2
Patient, treatment and tumor characteristics.

	N = 25
Age, mean (SD)	44 (14)
Female, n (%)	9 (36)
Seizure, n (%)	15 (60)
Resection, n (%)	25 (100)
Histopathology, n (%)	
Astrocytoma <i>IDHwt</i>	5 (20)
Astrocytoma <i>IDHmut</i>	9 (36)
Oligodendroglioma	11 (44)
Radiotherapy, n (%)	
After primary surgery	2 (8)
After redo surgery	8 (33)
Unknown/Missing	1
Chemotherapy, n (%)	
Upfront	0
At progression/transformation	8 (33)
Unknown/Missing	1
Later tumor resection, n (%)	10 (40)
Progression during follow-up, n (%)	10 (40)
Malignant transformation during follow-up, n (%)	8 (32)
Significant contrast enhancement	1 (4)
Verified with histopathology	7 (28)
Deceased during follow-up, n (%)	3 (12)

Table 3
Imaging characteristics.

Energy, median (IQR)	0.0009 (0.0004–0.0010)
Entropy, median (IQR)	7.9 (7.2–8.0)
Homogeneity, median (IQR)	0.12 (0.09–0.13)
Inertia, median (IQR)	329 (213–514)
Correlation, median (IQR)	0.0010 (0.0009–0.0020)
Contrast enhancement, n (%)	
No	19 (76)
Patchy	5 (20)
Nodular	1 (4)
Ring-like	0
Corpus callosum involvement, n (%)	2 (8)
Tumor border, n (%)	
Absent	6 (24)
Vague	9 (36)
Conspicuous	10 (40)
Mass effect, n (%)	
No	17 (68)
Mild	7 (28)
Conspicuous	1 (4)
Main tumor side, n (%)	
Left	13 (52)
Right	12 (48)
Main lobe involved, (%)	
Frontal	12 (48)
Temporal	6 (24)
Insula	7 (28)
Eloquence ^a , n (%)	10 (40)
Tumor volume, median in ml (IQR)	27 (7–37)

IQR denotes interquartile range.

^a As defined by Chang et al. [42].

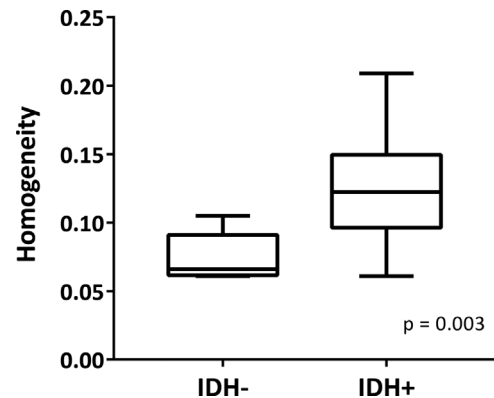


Fig. 1. Difference in homogeneity between patients with (median 0.12, IQR 0.10–0.15) and without (median 0.07, IQR 0.06–0.09) *IDH* mutation ($p = 0.005$). Whiskers show minimum and maximum value. There was a significant difference in homogeneity when comparing groups.

3.2. Radiology and malignant transformation

No significant correlation to hazard ratio for time to transformation was detected for either of the radiological parameters (data not shown).

4. Discussion

This exploratory study shows that quantitative radiological parameters from routine MRI scans were able to separate *IDHmut* and *IDHwt* in LGGs. The texture marker of homogeneity was the most promising, and together with LGG volume good diagnostic capabilities were demonstrated.

The use of Haralick texture parameters for diagnostic classification of tumors has been studied for several cancer types. The homogeneity parameter, also known as “inverse difference moment”, is a comparison of the signal intensity levels dispersed in the volume. A volume with smaller differences in MRI signal between neighboring voxels will result

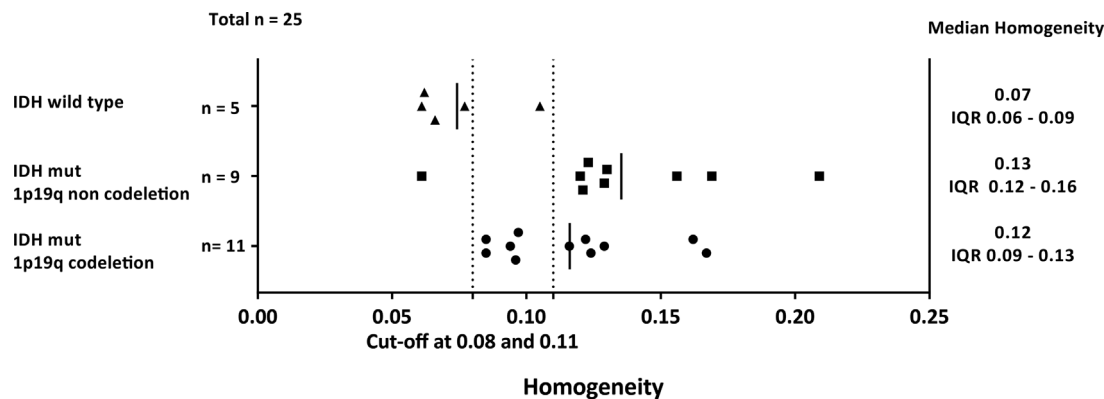


Fig. 2. Presentation of individual patients MRI FLAIR homogeneity in relation to molecular status, example cut-offs are given at 0.08 and 0.11.

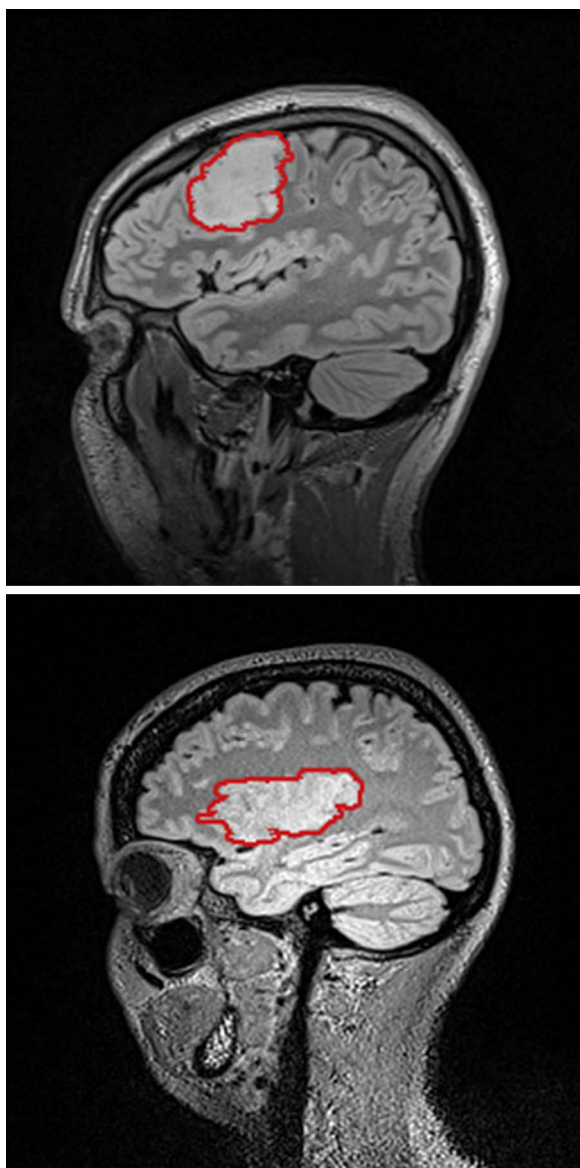


Fig. 3. Tumor with high homogeneity, 0.202 (upper) and low homogeneity, 0.065 (lower).

in higher homogeneity compared to one with larger differences, thus allowing quantification of tumor homogeneity/heterogeneity. Homogeneity has previously been used to identify mutation status in lung cancer [20] and to predict response to chemotherapy in breast

cancer [21].

The results from our study suggest worse prognosis for tumors with lower homogeneity (i.e. high tumor heterogeneity). This has also been seen in other studies of determining cancer prognosis through textural tumor heterogeneity [22–24]. Interestingly another recent study also reports that textural homogeneity is significantly lower in LGG patients with *IDHwt* compared to those with *IDHmut* [13]. This is also in line with findings of increased MRI heterogeneity in high-grade gliomas since *IDHwt* LGG much resembles high-grade gliomas from a biological point of view [11]. The cause of the higher heterogeneity has been suggested to be hypoxia or tumor angiogenesis [22,25]. Based on the aggressive clinical course of *IDHwt* LGG, these are also expected from a biological perspective to exhibit higher heterogeneity [14]. However, to establish a definite relationship between LGG mutation status, biological heterogeneity and radiological textural homogeneity prospective validation studies are needed.

Tumor growth rate in LGG has been the most consistent radiological prognostic marker [26]. Growth rate is associated with molecular classification since 1p19q codeleted LGG demonstrate slower growth rates [27]. Still, estimations of growth rate requires several scans with potential treatment delay and given that *IDHwt* tumors hold prognosis similar to glioblastomas, any delay should be avoided. Hence, separating LGGs at time of radiological diagnosis into either likely *IDHwt* or *IDHmut* is of a practical clinical value.

Other recent reports have presented approaches to predict molecular status in LGG [12,13,28,29–31,32]. A recent study analyzed the oncometabolite 2-hydroxyglutarate (2HG) by the means of MR spectroscopy in the clinical setting, and with a threshold of 2 mM 2HG the AUC was 0.88 for detection of *IDHmut* [28]. MR spectroscopy with monitoring of 2HG can also be used to monitor treatment response and tumor progression in *IDHmut* gliomas [32]. There is also a report on dynamic changes in textural homogeneity in relation to tumor response in lung cancer patients [23]. However, whether quantitative markers from routine MRI sequences can be used to monitor the course of the disease/treatment response remains to be seen.

Mazurowski and co-authors analyzed the shape of the tumor on FLAIR images and found that *IDHwt* had a more irregular shape, but with sensitivity limited to only 80% [29]. Nevertheless, this observation was supported by Yu et al., concluding that “[...] the tumor with *IDH1* mutation presents as more compact, more spherical and more rounded than the one with wild-type *IDH1*” [13]. Thus, this may at least serve as a simple, clinically detectable, sign of *IDH* mutation status.

Others have again used more advanced MRI techniques including techniques for perfusion, diffusion, oxygen metabolism and neovascularization [30,31]. Apparent diffusion coefficient (ADC) was more promising than relative cerebral blood volume (rCBV) in separating *IDHmut* from *IDHwt* due to large overlap in the rCBV values [30]. However, a model with a combination of rCBV, ADC value, tumor volume and contrast enhancement was promising with an AUC of 0.84.

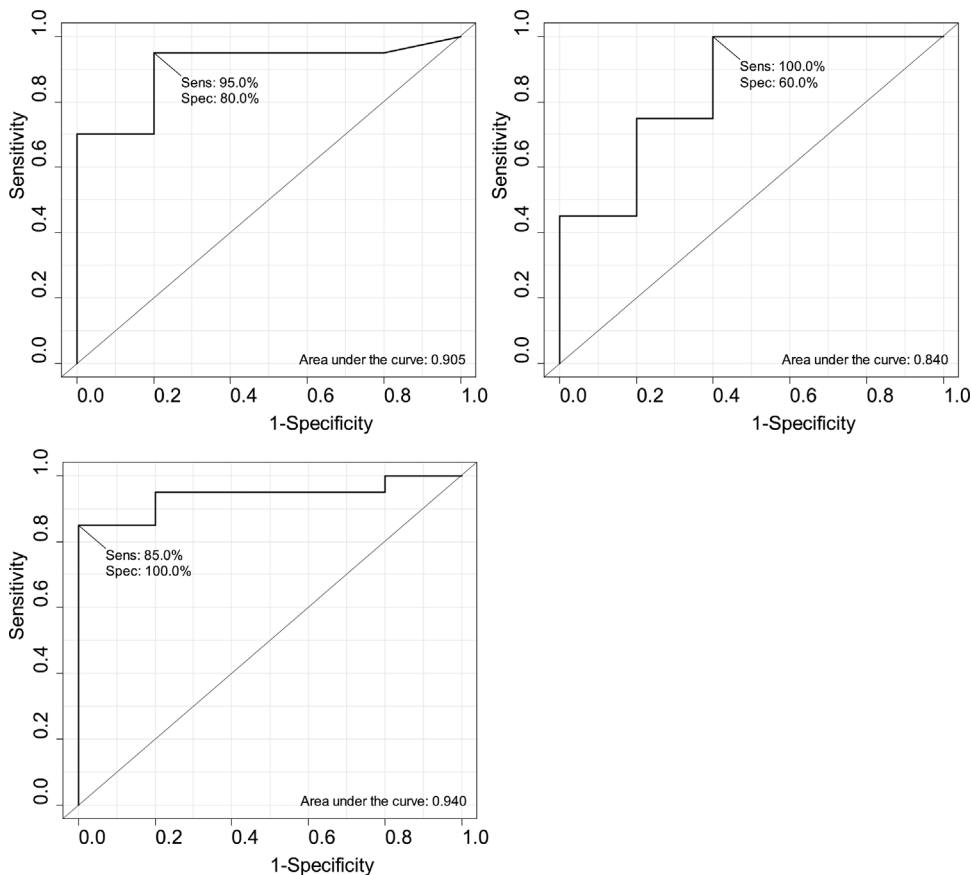


Fig 4. ROC curves for *IDH* mutation status correlated to homogeneity (upper left), tumor volume (upper right) and a logistic regression of a generalized linear model combining homogeneity and tumor volume (lower left).

However, when excluding anaplastic gliomas and analyzing LGG separately, the model only had AUC of 0.74 and 75% sensitivity of detecting *IDHmut*. Thus, the complexity of that model in light of the moderate diagnostic properties is likely to limit its clinical usefulness [30]. Similar to our study, tumor volume is associated with molecular class where *IDHmut* tend to be larger than *IDHwt* LGGs, but the overlap was too large to use this as the only radiological parameter [30]. Finally, cerebral metabolic rate of oxygen has been reported to be lower in *IDHmut* LGG [31]. However, the diagnostic capabilities from quantitative texture analyses in routine FLAIR images, without any additional scanning time, seems comparable to or more promising than other and more advanced techniques. This is also supported by two recently published and partly overlapping studies, where AUC of 0.916 and 94% sensitivity for detection of *IDH1* mutation was achieved using deep learning radiomics [12,13]. These numbers are comparable to our findings and should encourage further studies, and efforts should be used to overcome the barrier of standardized MR parameters to have broader clinical impact. Deep learning using large data may prove to be a valuable method in this regard [12,33].

Another technology that may facilitate quantitative radiology in the analysis of brain tumors is the emergence of synthetic MRI [34]. Synthetic MRI values can be standardized in retrospect, which opens up to easier application of quantitative radiology reducing scanner and parameter variability that currently limit the clinical usefulness of quantitative radiology today [34]. However, it remains to be seen if the artifacts more often observed in T2 and FLAIR images obtained from synthetic MRI data will hamper its use in LGG [34].

After the WHO 2016 classification incorporating molecular markers in glioma classification, interobserver variability in glioma subclassification is likely much reduced [2]. A reliable label (i.e. biological profile) is likely to improve radiological predictive models. There is now sufficient evidence to demonstrate the feasibility of radiogenomics also for LGG patients, indicating that imaging can potentially become

an important supplement to molecular analysis for hybrid classification [29,35]. For *IDH* classification, this hybrid is of lesser relevance since *IDH* mutation is an early common event with homogenous distribution throughout the tumor volume, but for other molecular events the intratumor heterogeneity is tremendous and radiology can thus provide important information of a much larger volume than typical biopsies [36–39].

5. Limitations

Due to the current limitations with respect to standardization of scan parameters, our study is just preliminary without any validation cohort. As this barrier may be reduced in the near future by the possibility of post-hoc scan adjustment, our preliminary results are very encouraging and should stimulate further research. It should be noted that some studies using homogeneity as textural parameter use a different mathematical formula that has similar properties but is not directly comparable to the one used in our study [22,40,41]. This highlights the difficulty in making direct comparisons between studies until consensus on which mathematical formula to use is achieved. Finally, a direct comparison with other potential valuable techniques for radiogenomics, such as MR spectroscopy or diffusion weighted images, was not performed since these exams were either lacking or non-standardized (e.g. different scanners and different hospitals).

In conclusion, this study indicates that quantitative radiology is promising in the determination of *IDH* molecular status in LGG. The capability of the texture variable homogeneity to separate *IDHmut* from *IDHwt* seems comparable or even more promising than most reported radiogenomic parameters to date.

Funding details

This work was supported by the The Norwegian Cancer Society; under Grant 5703787; Agreement concerning research and education of doctors under Grant ALFGBG-695611.

Disclosure statement

The authors report no conflicts of interest.

Acknowledgement

None.

References

- A.S. Jakola, K.S. Myrmed, R. Kloster, et al., Comparison of a strategy favoring early surgical resection vs a strategy favoring watchful waiting in low-grade gliomas, *JAMA* 25 (October) (2012) 1–8, <http://dx.doi.org/10.1001/jama.2012.12807> [pii] PubMed PMID: 23099483 Eng.
- D.N. Louis, A. Perry, G. Reifenberger, et al., The 2016 World Health Organization classification of tumors of the central nervous system: a summary, *Acta Neuropathol.* 131 (June (6)) (2016) 803–820, <http://dx.doi.org/10.1007/s00401-016-1545-1> PubMed PMID: 27157931; eng.
- D.J. Brat, R.G. Verhaak, K.D. Aldape, et al., Comprehensive, integrative genomic analysis of diffuse lower-grade gliomas, *N. Engl. J. Med.* 372 (June (26)) (2015) 2481–2498, <http://dx.doi.org/10.1056/NEJMoa1402121> PubMed PMID: 26061751 PubMed Central PMCID: PMCPCMC4530011. eng.
- R.J. Gillies, P.E. Kinahan, H. Hricak, Radiomics images are more than pictures, they are data, *Radiology* 278 (February (2)) (2016) 563–577, <http://dx.doi.org/10.1148/radiol.2015151169> PubMed PMID: 26579733 PubMed Central PMCID: PMCPCMC4734157. eng.
- H.J. Aerts, E.R. Velazquez, R.T. Leijenaar, et al., Decoding tumour phenotype by noninvasive imaging using a quantitative radiomics approach, *Nat. Commun.* 5 (2014) 4006, <http://dx.doi.org/10.1038/ncomms5006> PubMed PMID: 24892406; PubMed Central PMCID: PMCPCMC4059926. eng.
- B.M. Ellingson, M.G. Malkin, S.D. Rand, et al., Volumetric analysis of functional diffusion maps is a predictive imaging biomarker for cytotoxic and anti-angiogenic treatments in malignant gliomas, *J. Neurooncol.* 102 (March (1)) (2011) 95–103, <http://dx.doi.org/10.1007/s11060-010-0293-7> PubMed PMID: 20798977 PubMed Central PMCID: PMCPCMC3033973. eng.
- E.I. Zacharaki, N. Morita, P. Bhatt, et al., Survival analysis of patients with high-grade gliomas based on data mining of imaging variables, *AJNR Am. J. Neuroradiol.* 33 (June (6)) (2012) 1065–1071, <http://dx.doi.org/10.3174/ajnr.A2939> PubMed PMID: 22322603; PubMed Central PMCID: PMCPCMC4373623. eng.
- K.E. Emblem, M.C. Pinho, F.G. Zollner, et al., A generic support vector machine model for preoperative glioma survival associations, *Radiology* 275 (April (1)) (2015) 228–234, <http://dx.doi.org/10.1148/radiol.14140770> PubMed PMID: 25486589 eng.
- L. Macyszyn, H. Akbari, J.M. Pisapia, et al., Imaging patterns predict patient survival and molecular subtype in glioblastoma via machine learning techniques, *Neuro Oncol.* 18 (March (3)) (2016) 417–425, <http://dx.doi.org/10.1093/neuonc/nov127> PubMed PMID: 26188015; PubMed Central PMCID: PMCPCMC4767233. eng.
- B. Zhang, K. Chang, S. Ramkissoon, et al., Multimodal MRI features predict isocitrate dehydrogenase genotype in high-grade gliomas, *Neuro Oncol.* (June) (2016), <http://dx.doi.org/10.1093/neuonc/now121> PubMed PMID: 27353503; Eng.
- K. Skogen, A. Schulz, J.B. Dormagen, et al., Diagnostic performance of texture analysis on MRI in grading cerebral gliomas, *Eur. J. Radiol.* 85 (April (4)) (2016) 824–829, <http://dx.doi.org/10.1016/j.ejrad.2016.01.013> PubMed PMID: 26971430 eng.
- Z. Li, Y. Wang, J. Yu, et al., Deep learning based radiomics (DLR) and its usage in noninvasive IDH1 prediction for low grade glioma, *Sci. Rep.* 7 (July (1)) (2017) 5467, <http://dx.doi.org/10.1038/s41598-017-05848-2> PubMed PMID: 28710497 PubMed Central PMCID: PMCPCMC5511238. eng.
- J. Yu, Z. Shi, Y. Lian, et al., Noninvasive IDH1 mutation estimation based on a quantitative radiomics approach for grade II glioma, *Eur. Radiol.* 27 (August (8)) (2017) 3509–3522, <http://dx.doi.org/10.1007/s00330-016-4653-3> PubMed PMID: 28004160 eng.
- A.S. Jakola, A.J. Skjulsvik, K.S. Myrmed, et al., Surgical resection versus watchful waiting in low-grade gliomas, *Ann. Oncol.* (2017), <http://dx.doi.org/10.1093/annonc/mdx230> PubMed PMID: 28475680 eng.
- M.J. van den Bent, J.S. Wefel, D. Schiff, et al., Response assessment in neuro-oncology (a report of the RANO group): assessment of outcome in trials of diffuse low-grade gliomas, *Lancet Oncol.* 12 (June (6)) (2011) 583–593, [http://dx.doi.org/10.1016/S1470-2045\(11\)70057-2](http://dx.doi.org/10.1016/S1470-2045(11)70057-2) PubMed PMID: 21474379.
- H.K. Bo, O. Solheim, A.S. Jakola, et al., Intra-rater variability in low-grade glioma segmentation, *J. Neurooncol.* (November) (2016), <http://dx.doi.org/10.1007/s11060-016-2312-9> PubMed PMID: 27837437; Eng.
- R.M. Haralick, Statistical and structural approaches to texture, *Proc. IEEE* 67 (5) (1979) 786–804, <http://dx.doi.org/10.1109/PROC.1979.11328>.
- R.W. Connors, M.M. Trivedi, C.A. Harlow, Segmentation of a high-resolution urban scene using texture operators, *Comput. Vision Graphics Image Process.* 25 (3) (1984) 273–310, [http://dx.doi.org/10.1016/0734-189X\(84\)90197-X](http://dx.doi.org/10.1016/0734-189X(84)90197-X).
- C.A. Schneider, W.S. Rasband, K.W. Eliceiri, NIH Image to ImageJ: 25 years of image analysis, *Nat. Methods* 9 (July (7)) (2012) 671–675 PubMed PMID: 22930834 PubMed Central PMCID: PMCPCMC5554542. eng.
- E. Ozkan, A. West, J.A. Dedelow, et al., CT gray-level texture analysis as a quantitative imaging biomarker of epidermal growth factor receptor mutation status in adenocarcinoma of the lung, *Am. J. Roentgenol.* 205 (5) (2015) 1016–1025, <http://dx.doi.org/10.2214/AJR.14.14147> 2015/11/01.
- N. Michoux, S. Van den Broeck, L. Lacoste, et al., Texture analysis on MR images helps predicting non-response to NAC in breast cancer, *BMC Cancer* 05 (August (15)) (2015) 574, <http://dx.doi.org/10.1186/s12885-015-1563-8> PubMed PMID: 26243303 PubMed Central PMCID: PMCPCMC4526309. eng.
- F. Tixier, C.C. Le Rest, M. Hatt, et al., Intratumor heterogeneity characterized by textural features on baseline 18F-FDG PET images predicts response to concomitant radiochemotherapy in esophageal cancer, *J. Nucl. Med.* 52 (March (3)) (2011) 369–378, <http://dx.doi.org/10.2967/jnumed.110.082404>.
- G.J.R. Cook, M.E. O'Brien, M. Siddique, et al., Non-small cell lung cancer treated with erlotinib: heterogeneity of 18F-FDG uptake at PET—association with treatment response and prognosis, *Radiology* 276 (3) (2015) 883–893, <http://dx.doi.org/10.1148/radiol.2015141309> PubMed PMID: 25897473.
- S.C. Chan, K.P. Chang, Y.D. Fang, et al., Tumor heterogeneity measured on F-18 fluorodeoxyglucose positron emission tomography/computed tomography combined with plasma Epstein-Barr Virus load predicts prognosis in patients with primary nasopharyngeal carcinoma, *The Laryngoscope* 127 (January (1)) (2017) E22–E28, <http://dx.doi.org/10.1002/lary.26172> PubMed PMID: 27435352; eng.
- B. Ganeshan, V. Goh, H.C. Mandeville, et al., Non-small cell lung cancer: histopathologic correlates for texture parameters at CT, *Radiology* 266 (January (1)) (2013) 326–336, <http://dx.doi.org/10.1148/radiol.12112428> PubMed PMID: 23169792 eng.
- J. Pallud, M. Blonski, E. Mandonnet, et al., Velocity of tumor spontaneous expansion predicts long-term outcomes for diffuse low-grade gliomas, *Neuro Oncol.* (February) (2013), <http://dx.doi.org/10.1093/neuonc/nos331> nos331 [pii] [doi]. PubMed PMID: 23393207; Eng.
- C. Goze, C. Bezzina, E. Goze, et al., 1P19Q loss but not IDH1 mutations influences WHO grade II gliomas spontaneous growth, *J. Neurooncol.* 108 (May (1)) (2012) 69–75, <http://dx.doi.org/10.1007/s11060-012-0831-6> (PubMed PMID: 22392125 eng).
- A. Tietze, C. Choi, B. Mickey, et al., Noninvasive assessment of isocitrate dehydrogenase mutation status in cerebral gliomas by magnetic resonance spectroscopy in a clinical setting, *J. Neurosurg.* (March) (2017) 1–8, <http://dx.doi.org/10.3171/2016.10.jns161793> PubMed PMID: 28298040 eng.
- M.A. Mazurowski, K. Clark, N.M. Czarnek, et al., Radiogenomics of lower-grade glioma: algorithmically-assessed tumor shape is associated with tumor genomic subtypes and patient outcomes in a multi-institutional study with the cancer genome atlas data, *J. Neurooncol.* (May) (2017), <http://dx.doi.org/10.1007/s11060-017-2420-1> PubMed PMID: 28470431; eng.
- K. Leu, G.A. Ott, A. Lai, et al., Perfusion and diffusion MRI signatures in histologic and genetic subtypes of WHO grade II–III diffuse gliomas, *J. Neurooncol.* (May) (2017), <http://dx.doi.org/10.1007/s11060-017-2506-9> PubMed PMID: 28547590 eng.
- A. Stadlbauer, M. Zimmermann, M. Kitzwogger, et al., MR imaging-derived oxygen metabolism and neovascularization characterization for grading and IDH gene mutation detection of gliomas, *Radiology* 283 (June (3)) (2017) 799–809, <http://dx.doi.org/10.1148/radiol.2016161422> PubMed PMID: 27982759 eng.
- C. Choi, J.M. Raisanen, S.K. Ganji, et al., Prospective longitudinal analysis of 2-Hydroxyglutarate magnetic resonance spectroscopy identifies broad clinical utility for the management of patients with IDH-mutant glioma, *J. Clin. Oncol.* 34 (November (33)) (2016) 4030–4039, <http://dx.doi.org/10.1200/jco.2016.67.1222> PubMed PMID: 28248126 eng.
- Y. LeCun, Y. Bengio, G. Hinton, Deep learning, *Nature* 521 (May (7553)) (2015) 436–444, <http://dx.doi.org/10.1038/nature14539> PubMed PMID: 26017442 eng.
- L.N. Tanenbaum, A.J. Tsiouris, A.N. Johnson, et al., Synthetic MRI for clinical neuroimaging: results of the magnetic resonance image compilation (MAGiC) prospective, multicenter, multireader trial, *AJNR Am. J. Neuroradiol.* 38 (June (6)) (2017) 1103–1110, <http://dx.doi.org/10.3174/ajnr.A5227> PubMed PMID: 28450439 eng.
- K. Aldape, M.L. Simmons, R.L. Davis, et al., Discrepancies in diagnoses of neuroepithelial neoplasms, *Cancer* 88 (10) (2000) 2342–2349, [http://dx.doi.org/10.1002/\(sici\)1097-0142\(20000515\)88:10<2342:aid-ncr19>3.0.co;2-x](http://dx.doi.org/10.1002/(sici)1097-0142(20000515)88:10<2342:aid-ncr19>3.0.co;2-x).
- A. Sottoriva, I. Spiteri, S.G. Piccirillo, et al., Intratumor heterogeneity in human glioblastoma reflects cancer evolutionary dynamics, *Proc. Natl. Acad. Sci. U. S. A.* 110 (March (10)) (2013) 4009–4014, <http://dx.doi.org/10.1073/pnas.1219747110> [pii]. PubMed PMID: 23412337; PubMed Central PMCID: PMC3593922. eng.
- H. Suzuki, K. Aoki, K. Chiba, et al., Mutational landscape and clonal architecture in grade II and III gliomas, *Nat. Genet.* 47 (May (5)) (2015) 458–468, <http://dx.doi.org/10.1038/ng.3273> PubMed PMID: 25848751; eng.
- N.J. Szerlip, A. Pedraza, D. Chakravarty, et al., Intratumoral heterogeneity of receptor tyrosine kinases EGFR and PDGFR amplification in glioblastoma defines subpopulations with distinct growth factor response, *Proc. Natl. Acad. Sci. U. S. A.* 109 (February (8)) (2012) 3041–3046, <http://dx.doi.org/10.1073/pnas.1114033109> [pii]. PubMed PMID: 22323597; PubMed Central PMCID: PMC3286976. eng.
- N. Andor, T.A. Graham, M. Jansen, et al., Pan-cancer analysis of the extent and

- consequences of intratumor heterogeneity, *Nat. Med.* (November) (2015), <http://dx.doi.org/10.1038/nm.3984> PubMed PMID: 26618723; Eng..
- [40] D. Groheux, A. Martineau, L. Teixeira, et al., 18FDG-PET/CT for predicting the outcome in ER + /HER2- breast cancer patients: comparison of clinicopathological parameters and PET image-derived indices including tumor texture analysis, *Breast Cancer Res.* 19 (January (1)) (2017) 3, <http://dx.doi.org/10.1186/s13058-016-0793-2>.
- [41] M. Nakajo, M. Jinguji, M. Nakajo, et al., Texture analysis of FDG PET/CT for differentiating between FDG-avid benign and metastatic adrenal tumors: efficacy of combining SUV and texture parameters, *Abdom. Radiol.* (June) (2017), <http://dx.doi.org/10.1007/s00261-017-1207-3>.
- [42] E.F. Chang, J.S. Smith, S.M. Chang, et al., Preoperative prognostic classification system for hemispheric low-grade gliomas in adults, *J. Neurosurg.* 109 (5) (2008) 817–824, <http://dx.doi.org/10.3171/JNS.2008.109.11.0817> PubMed PMID: 18976070.